TECHNICAL TRANSACTIONS | CZASOPISMO TECHNICZNE
MECHANICS | MECHANIKA
1-M/2016

THOMAS BUDIARTO, ERIK ESCHE, JENS-UWE REPKE*

DYNAMIC MODELLING AND OPERATION OF THE CHLOR-ALKALI PROCESS

MODELOWANIE I STEROWANIE PROCESEM ELEKTROLIZY CHLORKU SODU

Abstract

Chlorine it is commonly produced through the Chlor-alkali process, which is an electrochemical process – the process energy consumption dominates the production cost. Therefore, optimization of the process has become a major issue to achieve energy conservation and cost effective production. This study aims at investigating the transient and steady-state behavior of the chlorine production system through process modeling and simulation. Material balance and energy balance of the Chlor-alkali membrane process (electrolysis), brine pre-treatment, and chlorine handling are modelled and investigated using rigorous models. MOSAIC and MATLAB, are used to model and to simulate the process response when receiving dynamic input. For validation, the simulation result is compared to experimental data.

Keywords: chlor-alkali membrane process, dynamic model, electrochemical cell

Streszczenie

Chlor wytwarzany jest powszechnie w procesie elektrolizy chlorków metali alkalicznych – energochłonność procesu dominuje koszt produkcji. Dlatego optymalizacja procesu stała się poważnym problemem. Celem pracy było zbadanie i modelowanie procesu produkcji chloru w stadiach stacjonarnych i przejściowych. Bilanse materiałowy i energetyczny procesu membranowego (elektroliza), wstępna obróbka solanki i magazynowanie chloru zostały przetestowane przy użyciu rygorystycznych modeli. MOSAIC i MATLAB były wykorzystywane do modelowania i symulacji procesów odpowiedzi układu na dynamiczne wymuszenie. Dla weryfikacji wyniki symulacji porównano z danymi doświadczalnymi.

Słowa kluczowe: proces membranowy, przemysł chloro-alkaiczny, model dynamiczny, ogniwo elektrochemiczne

DOI:

* MSc. Thomas Budiarto, DSc. Eng. Erik Esche, Prof. PhD. DSc. Eng. Jens-Uwe Repke, Process Dynamics and Operations Group, Faculty Of Process Sciences, Technical University of Berlin.

1. Introduction

By now, renewable energy has become an important component of Germany's energy mix. In 2014, renewable sources amounted to 26.2% of power generation, and this is increasing further due to the German Government requiring the renewable energy share in power generation to reach 40÷45% by 2025 and 55÷60% by 2035 [14].

Chlorine is one of the most indispensable intermediates in the chemical industry. It is commonly produced through the chlor-alkali process, which is an electrochemical process that decomposes an aqueous solution of sodium chloride by direct current, producing chlorine gas, hydrogen gas, and sodium hydroxide solution. The process's energy consumption dominates the production cost. Given the large-scale introduction of renewable energy sources in Germany's electrical grid, both energy suppliers as well as consumers have to adjust to an increasingly flexible market. Therefore, optimisation of the process has become a major issue to achieve energy conservation and cost effective production. It is important to understand the dynamic and steady-state behaviour of the process in order to optimize the process operation relating to plant energy consumption.

In order to understand the demand response potential of the chlor-alkali process, the dynamic response of the process is modelled. The Butler-Volmer equation and the Nernst equation are used to model the dynamic behaviour of the current density and chlorine production rate. Both of these equations correlate the material balance with the energy consumption of the process.

2. The Process Model

In order to investigate the dynamics of the energy consumption of the chlor-alkali process, a material balance model and an electrolytic cell voltage model were developed. The process consists of two half-cells, which are known as the anode cell and cathode cell. The chemical reactions which are considered in the developed model can be expressed as:

Anode cell : $2Na^+ + 2Cl^- \rightarrow Cl_2 + 2Na^+ + 2e^-$

$2Cl^- \rightarrow Cl_2 + 2e^-$

Cathode cell : $2H_2O + 2e^- \rightarrow H_{2(g)} + OH^-$

$Na^+ + OH^- \rightarrow NaOH_{(aq)}$

Total reaction : $2H_2O + 2NaCl \rightarrow H_{2(g)} + Cl_{2(g)} + 2NaOH_{(aq)}$

The developed model consists of a material balance model and dynamic model of the energy consumption regarding the dynamics of the material balance in the electrochemical cell. Fig. 1 illustrates the process which is modelled in this study.

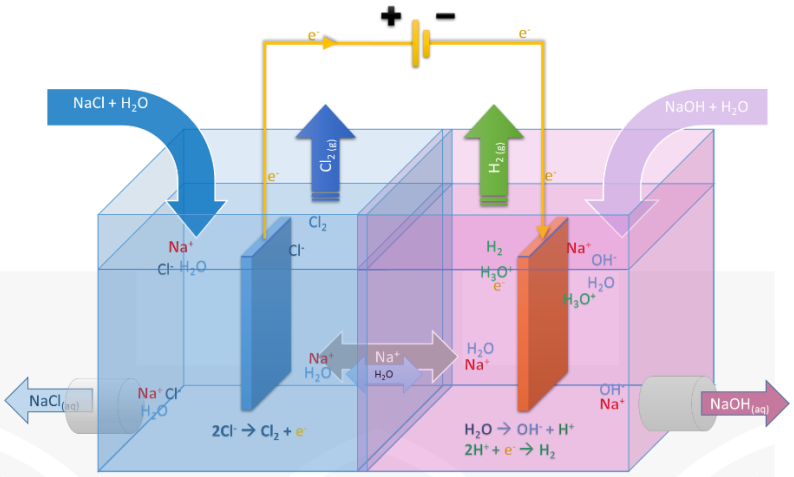

Fig. 1. Diagram of chlor-alkali model

The material balance model considers balances for sodium ions, hydroxide ions, water, and chloride. The liquid volume of each half cell is assumed to be constant and the concentrations of the electrolyte are distributed uniformly. In accordance with Faraday's Law, gas production rates in the chlor-alkali cell can be estimated using the following expressions:

$$\dot{N}_{CatOut}^{H_2} = \frac{i \cdot A}{2F} \tag{1}$$

$$\dot{N}_{CatOut}^{Cl_2} = \frac{i \cdot A}{2F} \tag{2}$$

In these expressions, the current efficiency for producing chlorine and hydrogen gas are assumed to be 100%. The other parallel reactions which appear to be current inefficiency problems are neglected in this model. Tilak and Chen [2] mention that chlorine gas in the anode might dissolve in water to form soluble chlorine, which hydrolyses to form HOCl and OCl^-. HOCl and OCl^- react further to form ClO_3^-. However, based on reference [3], the solubility of Chlorine in water and a solution of NaCl is below 1% of the solution weight when the solution temperature is above 20°C. In accordance with reference [3], Fig. 2 shows that the solubility of chlorine in water, HCl solution, and NaCl solution decreases with increases in temperature and concentration. Hence, the influence of this parallel reactions is minor compared to the other chlor-alkali reactions.

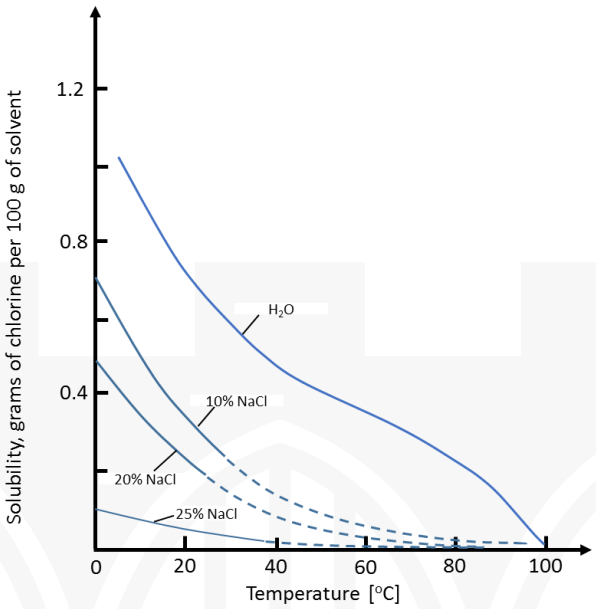

Fig. 2. Solubility of chlorine in water, hydrochloric acid, and sodium chloride solutions, in accordance with reference [3]

1.1. Material Balance Model

In the developed model, the process and ions transport between the anolyte and catholyte does not change the volume of either the catholyte or anolyte. The accumulative volume of the anolyte and catholyte are modelled as:

$$\frac{dV_{CatAcc}}{dt} = \dot{V}_{CatIn} - \dot{V}_{CatOut} \tag{3}$$

$$\frac{dV_{AnAcc}}{dt} = \dot{V}_{AnIn} - \dot{V}_{AnOut} \tag{4}$$

In the simulation, the accumulative volume of the catholyte and anolyte will be assumed to be constant. Both in the anode and cathode, the feed flow rate is equal to the outlet flow.

1.1.1. Sodium Ion Balance

Sodium ions in the modelled process mainly originate from NaCl in the anolyte feed. Some processes consider the feeding of lean concentrations of NaOH as a catholyte input in

order to gain higher NaOH concentration at the cathode outlet. The following equations (equations 5, 6 and 7) formulate the sodium ion balance in the cell.

$$\frac{dN_{CatAcc}^{Na}}{dt} = C_{CatIn}^{NaOH} \cdot \dot{V}_{CatIn} - C_{CatAcc}^{Na} \cdot \dot{V}_{CatOut} + \frac{A \cdot D^{Na}}{\delta} \cdot \left(C_{AnAcc}^{Na} - C_{CatAcc}^{Na}\right) \quad (5)$$

$$\frac{dN_{AnAcc}^{Na}}{dt} = C_{AnIn}^{NaCl} \cdot \dot{V}_{AnIn} - C_{AnAcc}^{Na} \cdot \dot{V}_{AnOut} - \frac{A \cdot D^{Na}}{\delta} \cdot \left(C_{AnAcc}^{Na} - C_{CatAcc}^{Na}\right) \quad (6)$$

$$C_{AnIn}^{Na} = \frac{N_{AnAcc}^{Na}}{V_{AnAcc}}; \; C_{CatIn}^{Na} = \frac{N_{CatAcc}^{Na}}{V_{CatAcc}} \quad (7)$$

Based on some references [13, 15, 16], the concentration gradient of solutions across a polymeric membrane contributes to material transport in the electrochemical cell. In reference [13], it is mentioned that the concentration gradient of water across a proton exchange membrane in a water electrolyser contributed to mass flow inside the cell. The developed sodium balance model also considers the concentration gradient as the driving force of Na^+ ion transport between anolyte and catholyte. In the developed model, the ion exchange rate is proportional to the ion diffusion area, the diffusion coefficient of Na^+ ions, and the concentration gradients between the anolyte and catholyte. Conversely, the exchange rate is inversely proportional to the membrane thickness.

1.1.2. Hydroxide Ion Balance

The hydroxide ions are produced by a cathode reaction which breaks down the water into OH^- and H^+ ions. Based on Faraday's Law, the OH^- production rate is proportional to the electrolysis current that drives the cathode reaction. The developed model also assumes that the ion-exchange membrane halts the hydroxide ions transfer from catholyte to anolyte. The OH^- ions then cease to exist in the anode compartment. The hydroxide ion balance can be written as:

$$\frac{dN_{CatAcc}^{OH}}{dt} = C_{CatIn}^{NaOH} \cdot \dot{V}_{CatIn} + \frac{i \cdot A_{el}}{2F} - \frac{N_{CatAcc}^{OH}}{V_{CatAcc}} \cdot \dot{V}_{CatOut} \quad (8)$$

1.1.2. Water Balance

In the developed model, concentration of water is also considered as it influences the cathode reaction potential. Water in the cathode mainly stems from the cathode feed. Some water molecules in the anode also move through the membrane to the cathode due to the concentration gradient between the anode and cathode [13, 15, 16]. The water balance in the anode and cathode is expressed as:

$$\frac{dN_{CatAcc}^{H_2O}}{dt} = (55.56 - C_{CatIn}^{NaOH}) \cdot \dot{V}_{CatIn} - C_{CatAcc}^{H_2O} \cdot \dot{V}_{CatOut} - \frac{A \cdot D^{H_2O}}{\delta} \cdot \left(C_{CatAcc}^{H_2O} - C_{AnAcc}^{H_2O}\right) \quad (9)$$

$$\frac{dN_{AnAcc}^{H_2O}}{dt} = (55.56 - C_{AnIn}^{NaCl}) \cdot \dot{V}_{AnIn} - C_{AnAcc}^{H_2O} \cdot \dot{V}_{AnOut} + \frac{A \cdot D^{H_2O}}{\delta} \cdot \left(C_{CatAcc}^{H_2O} - C_{AnAcc}^{H_2O}\right) \quad (10)$$

where :

D^{H_2O} – Diffusion coefficient of H_2O molecule in the membrane ($2 \cdot 10^{-10}$ m^2/s)[1].

1.1.2. Chloride Ion Balance

In the chlor-alkali cell, chloride ions enter with the anode feed, which is a NaCl solution. The chloride ions in the anolyte are consumed by the anode cell reaction to produce chlorine gas. The reaction rate is estimated by counting the rate of electrons transferred to the chloride ion in the anolyte – this is commonly known as the electric current. So, the developed material balance model describes accumulated chloride ions in the anolyte using the following expression:

$$\frac{dN_{AnAcc}^{Cl}}{dt} = C_{AnIn}^{NaCl} \cdot \dot{V}_{AnIn} - \frac{i \cdot A_{el}}{2F} - \frac{N_{AnAcc}^{Cl}}{V_{AnAcc}} \cdot \dot{V}_{AnOut} \quad (11)$$

1.2. Energy Consumption Model

The chlor-alkali process consumes electrical energy from an external power supply. Cell voltage is one of most important process variables that defines the energy consumption of the process. In the developed model, the required cell voltage is the accumulation of the following:

- standard electrode potential,
- activation overpotential,
- Ohmic overpotential drop in the membrane, electrolytes, electrodes and conductors.

This cell voltage model is described in the following equations:

$$V_{cell} = E + \mu_{act} + \mu_{ohm} \quad (12)$$

$$E = E_{An}^0 - E_{Cat}^0 + \frac{R \cdot T}{2 \cdot F \cdot \alpha} \left(ln\left(\frac{\sqrt{p_{an}^{Cl_2}}}{C_{AnAcc}^{Cl}} \right) - 0{,}5\, ln\left(\frac{\left(C_{CatAcc}^{H_2O}\right)^2}{p_{Cat}^{H_2} \cdot C_{CatAcc}^{OH}} \right) \right) \quad (13)$$

$$\mu_{act} = \frac{R \cdot T}{2 \cdot F \cdot \alpha} ln\left(\left(\frac{i}{2i_{an}^o} + \sqrt{\frac{i}{\left(2i_{an}^o + 1\right)^2}} \right) \left(\frac{i}{2i_{cat}^o} + \sqrt{\frac{i}{\left(2i_{cat}^o + 1\right)^2}} \right) \right) \quad (14)$$

$$\mu_{ohm} = i \cdot A \cdot R_{cell} \quad (15)$$

1.3. Modelling and Simulation Process

The overview modelling and simulation process is shown by Fig. 3. All of the model components are developed and integrated in the MOSAIC modelling environment. Then, the developed model is simulated in Matlab. The simulation results are discussed further in the subsequent subtitles.

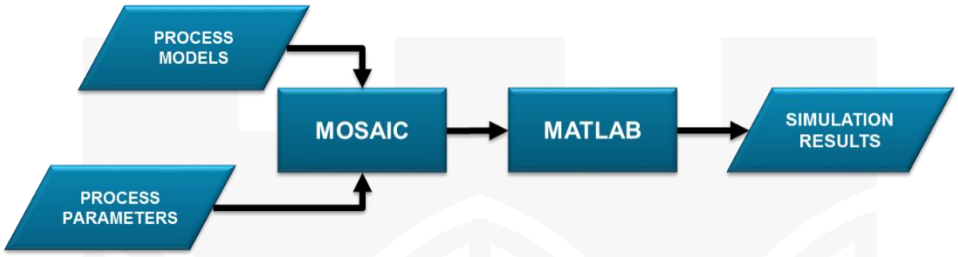

Fig. 3 Modelling and Simulation Process Diagram

3. Model Validation

A model validation is performed by comparing steady-state simulation data with experimental data provided by [4]. The model is constructed in MOSAIC and then simulated in Matlab.

Dias [4] measured some variables from a laboratory-scale chlor-alkali electrolyser to investigate and characterise the membrane cell. The comparison results are expressed in the Fig.4. It shows the polarisation curve of the chlor-alkali cell model and the chlor-alkali electrolyzer. These figures show that the polarization curves of both display a similar trend, although there is an offset between the model values and the experiment values.

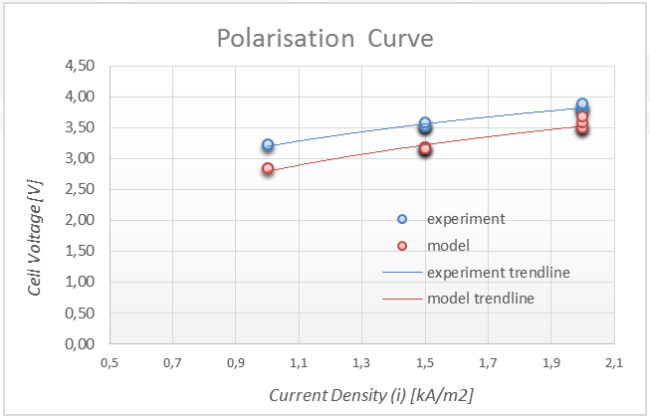

Fig. 4 Polarisation curve of chlor-alkali cell model and chlor-alkali cell electrolyzer

The offset emerges due to the fact that the cell voltage model does not consider the hydrodynamics inside the cell compartment. Some references [4, 6, 7, 8] mentioned that in the experimental cell, the existence of bubbles inside the cell compartment influences the cell voltage. Fig. 5(a) shows that cell voltage tends to increase when the gas void fraction increases – this also increases the difference between the cell voltage and its theoretical value.

Some references [4, 6, 9, 10, 11, 12] mentioned that at the same current density, increasing the volume rate through the cell compartment increases the electrolyte circulation and as a result, decreases the electrolyte resistance due to improved gas removal. As expected, the increase of the volume rate into the cell compartment tends to reduce the offset between the model and experimental data, as shown in Fig. 5(b).

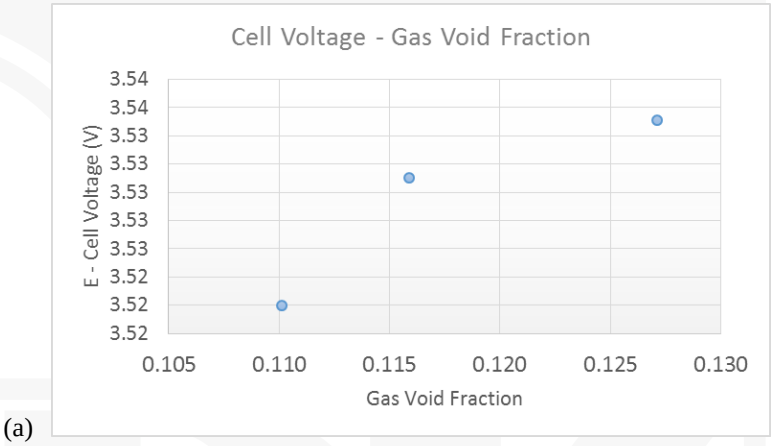

(a)

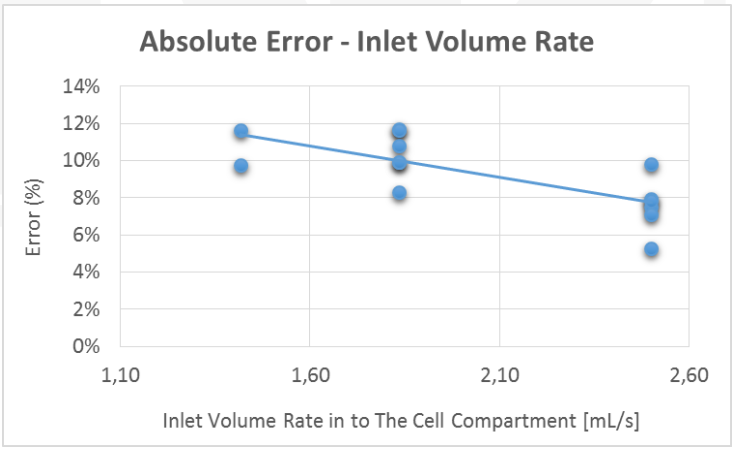

(b)

Fig. 5 (a) Cell voltage compared to gas void fraction; (b) Absolute error (model bias) compared to gas void fraction

4. Simulation

Simulations are performed to investigate the dynamic behaviour of the cell when the cell's voltage increases. In this simulation, operation voltage is increased from 0 V to 4 V. The cell is operated in voltage driven mode. The electrolyte volume during the simulation is kept constant. Inlet and outlet volume rates are also constant and have equal values. The simulation parameters are listed in table 1.

Table 1

Simulation Parameters

Process Parameter	Value
[NaCl] at anode inlet (kmol/m^3)	5
[NaOH] at cathode inlet (kmol/m^3)	10
A_{el} / Electrode effective area (m^2)	1
A / Membrane effective area (m^2)	1
$\dot{V}_{AnIn}$, $\dot{V}_{AnOut}$, $\dot{V}_{CatIn}$, $\dot{V}_{CatOut}$ (m^3/s)	$1\cdot10^{-3}$; $0.5\cdot10^{-3}$; $0.2\cdot10^{-3}$
V_{Cat}, V_{An} / volume anolyte and catholyte (m^3)	$5\cdot10^{-2}$
α	0.5
D^{Na}	$4\cdot10^{-9}$
D^{H2O}	$2\cdot10^{-10}$
$E^0_{An} - E^0_{Cat}$ (V)	2.2
V_{cell} (V)	4
R_{cell} (Ohm)	$7.33e^{-5}$
R (m^3.kPa/ K.kmol)	8.314
T (K)	363.0
i^0_{an} (kA/m^2)	$1\cdot10^{-10}$
i^0_{cat} (kA/m^2)	$3\cdot10^{-9}$
i / current density (kA/m^2)	0.5 – 2.0

Results of the simulation are shown by Fig. 6, Fig. 7, and Fig. 8. The results show that the process model is a 1st order dynamic system. These results are expected since material transport in the process, which has a1st order dynamic, has the longest time constant compared to the others processes in the electrolysis. Based on these results, it can be concluded that the material transport dictates the process kinetics. This can be seen in Fig.6, which displays current density charts for three different electrolyte circulation rate values (*Vdot*). The electrolyte circulation rate represents the inlet and outlet volume rate of electrolytes (*Vdot*) in the simulation.

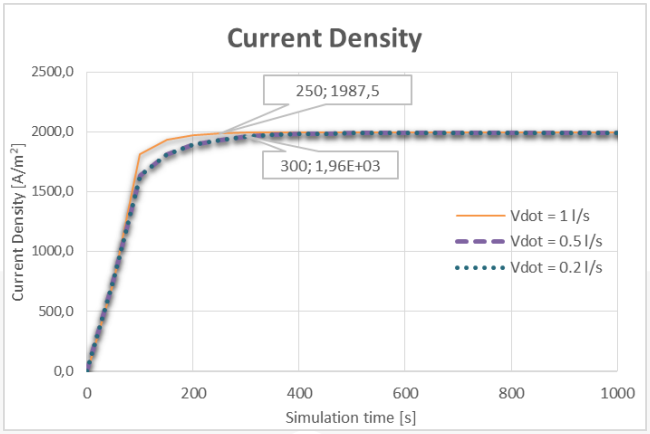

Fig. 6. Current density of simulated chlor-alkali membrane cell

Fig. 6 also shows that higher circulation rates shortens the process' response time. The process' settling time, the time for achieving a steady state, is 250 seconds for a circulation rate of 1 l/s. The settling time increases to 300 seconds for a lower circulation rate at 0.5 l/s.

Fig. 7 shows components of the cell's voltage during the simulation. The figure shows that the decomposition voltage (E) dominate the proportion of total cell voltage. The voltage's value at steady state is lower than its value in the initial condition. The voltage reduction occurs because in the steady state condition the relative activity of the reactants are higher compared to their relative activity at time point zero. The others voltage components, the activation and ohmic voltage, increase along with the increase of electrolysis current.

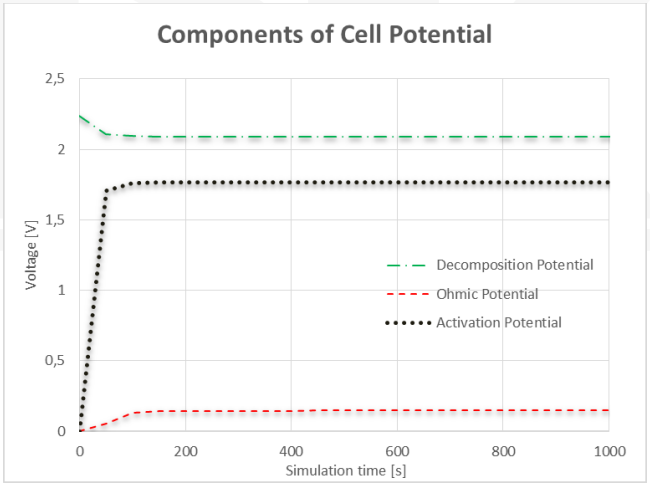

Fig. 7. Decomposition potential, activation potential and ohmic potential of chlor-alkali membrane cell, at $\dot{V} = 1\ l/s$

Fig. 8 displays the dynamic of the production rate of chlorine gas. The production rate is linear to the current density given that the current efficiency in the model is 100%.

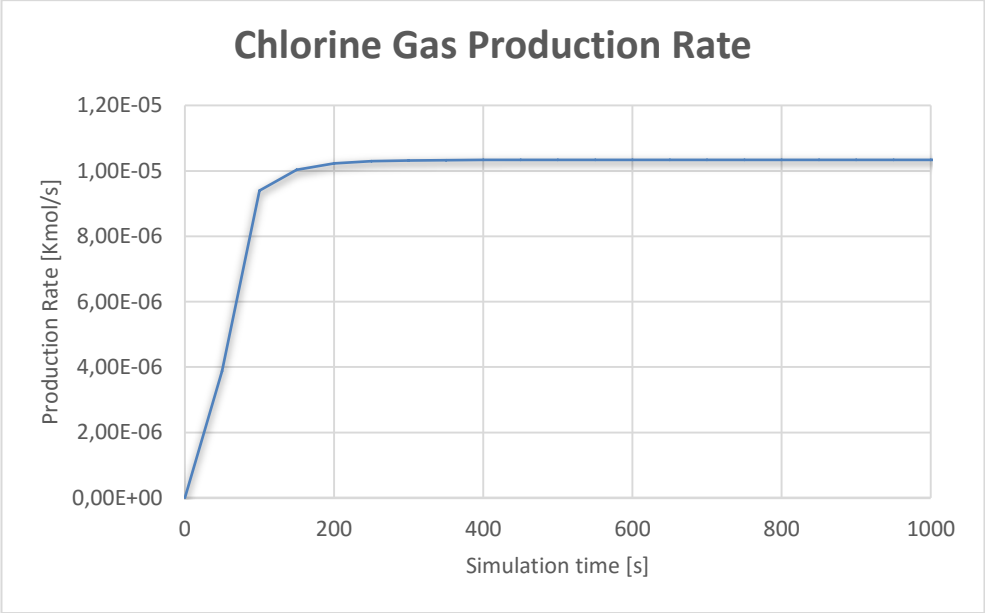

Fig. 8 Cl_2 gas production rate, at $\dot{V} = 1\ L/s$

5. Conclusion

In order to investigate the demand response potential of the chlor-alkali membrane process, a dynamic process model of the chlor-alkali membrane process has been developed in the MOSAIC modeling environment and solved in Matlab.

The model considers the dynamic behaviour of the material balance and the relationship between the cell voltage, current density, and ion concentrations in the electrolyte. For the validation, the model shows similar trends to experimental data. However, an offset exists in the voltage value predictions especially at high current density in comparison to lab-scale experimental data. This offset is caused by the simplification of the hydrodynamic behaviour in the model.

The simulation of the developed model shows that material transport dictates the process dynamics. The simulated process achieves steady state approximately after 250 seconds, which increases for lower reactant circulation rates.

For future work, it is important to include a current efficiency estimation model and an ohmic resistance model in the process model in order to achieve a more comprehensive description of the process' dynamic behaviour.

Nomenclature

$\dot{N}_{CatOut}^{H2}$ – production rate of H_2 in the cathode cell, kmol/s,

$\dot{N}_{AnOut}^{Cl2}$ – production rate of Cl_2 in the anode cell, kmol/s,

I – electrolysis current, kA

F – faraday constant : 96'485, kCoulomb/kmol·e,)

V_{CatAcc} – accumulative volume of catholyte, m^3,

$\dot{V}_{CatIn}$ – volume rate of cathode inlet, m^3/s,

$\dot{V}_{CatOut}$ – volume rate of cathode outlet, m^3/s,

$\dot{V}_{AnIn}$ – volume rate of anode inlet, m^3/s,

$\dot{V}_{AnOut}$ – volume rate of anode outlet, m^3/s,

N_{CatAcc}^{Na}, N_{AnAcc}^{Na} – mole quantity of Na^+ ion in catholyte and anolyte, kmol,

C_{CatIn}^{NaOH} – concentration of NaOH in the catholyte feed, kmol/m^3,

C_{AnIn}^{NaCl} – concentration of NaCl in the anolyte feed, kmol/m^3,

C_{AnAcc}^{Na} – concentration of Na^+ ion in the anolyte, kmol/m^3,

C_{CatAcc}^{Na} – concentration of Na^+ ion in the catholyte, kmol/m^3,

$\dot{V}_{CatIn}$, $\dot{V}_{AnIn}$ – feeding rate in the cathode and anode compartment, m^3/s,

$\dot{V}_{CatOut}$, $\dot{V}_{AnOut}$ – outlet rate of the cathode and anode compartment, m^3/s,

A – ion diffusion area in the membrane, 10^{-2} m^2,

D^{Na} – diffusion coefficient of Na^+ ion in the membrane, $4 \cdot 10^{-9} m^2/s$ [1],

δ – membrane thickness, $2.5 \cdot 10^{-4}$ m [4],

N_{CatAcc}^{OH} – mole quantity of OH^- ion, kmol,

C_{CatIn}^{NaOH} – concentration of NaOH in the catholyte feeding, kmol/m^3,

$\dot{V}_{CatIn}$ – feeding rate in the cathode compartment, m^3/s,

$\dot{V}_{CatOut}$ – outlet rate of the cathode compartment, m^3/s,

N_{AnAcc}^{Cl} – accumulated Cl^- ion in the anode, kmol,

C_{AnIn}^{NaCl} – concentration of NaCl in the anode feeding, kmol/m^3,

$\dot{V}_{AnIn}$ – feeding rate in the anode, m^3/s,

$\dot{V}_{AnOut}$ – outlet rate of the anode, m^3/s,

V_{cell} – cell voltage, Volt,

E – standard electrode potential, Volt,

μ_{act} – activation overpotential, Volt,

μ_{ohm} – Ohmic overpotential, Volt,

$E_{An}^0 - E_{Cat}^0$ – standar electrode potential for anode and cathode, Volt,

α – charge transfer coefficient, symmetry factor = 0.5,

T – temperature, K,
R – ideal gas constant: 0.008314, $m^3 \cdot Pa/(K \cdot kmol)$,
i – current density, kA/m^2,
i_{an}^0 – exchange current density of anode, $1 \cdot 10^{-10}$ kA/m^2,
i_{cat}^0 – exchange current density of cathode, $3 \cdot 10^{-9}$ kA/m^2.

References

[1] Friedfeld B.A. (author), Wellington T.C. (editor), *Modern Chlor-Alkali Technology*, vol. 5, Springer Netherlands 1992.
[2] TILAK B.V., Chen C.-P., *Calculation of the current efciency of the electrolytic sodium chlorate cells*, Journal of Applied Electrochemistry, vol. 29, 1999, 1237-1240.
[3] Schmittinger P., Florkiewicz T., Curlin L.C., Luke B., et.al., *Ullmann's Encyclopedia of Industrial Chemistry – Chlorine*, Wiley-VCH Verlag GmbH & Co. KGaA, Weinheim 2012.
[4] Dias, A.C.d.B.V., *Chlor-Alkali Membrane Cell Process*, PhD Disertation, Chemical and Biological Engineering – University of Porto 2013.
[5] Hardee K.L., *A Simple procedure for evaluating membrane electrolyzer performance*, Modern Chlor-Alkali Technology, vol. 6, 1995, 235-242.
[6] Hine F., Yasuda M., Nakamura R., Noda T., Journal of The Electrochemical Society vol. 122, 1975, 1185-1190.
[7] Xiong Y., Jialing L., Hong S., Journal of Applied Electrochemistry, vol. 22, 1992, 486-490,.
[8] Mandin Ph., Aissa A., Roustan H., Hamburger J., Picard G., Chemical Engineering and Processing, vol. 47, 2008, 1926-1932.
[9] Mirzazadeh T., Mohammadi F., Soltanieh M., Joudaki E., Chemical Engineering Journal, vol. 140, 2008, 157-164.
[10] Kaveh N. S., Ashrafizadeh S.N., Mohammadi F., Chemical Engineering Research and Design, vol. 86, 2008, 461-472.
[11] Jalali A.A., Mohammadi F., Ashrafizadeh S.N., Desalination, vol. 237, 2009, 126-139.
[12] Kaveh N. S., Mohammadi F., Ashrafizadeh S.N., Chemical Engineering Journal, vol 147, 2009, 161–172.
[13] Marangio F., Santarelli M., Calı` M., *Theoretical model and experimental analysis of a high pressure PEM water electrolyser for hydrogen production*, International Journal of Hydrogen Energy, vol. 34, 2009, 1143-1158.
[14] Auer, J., Anatolitis, V., *The Changing energy mix in Germany*. Deutche Bank Research, Curent Issues – Natural Resources, June 26, 2014.
[15] Bird R.B., Stewart W.E., Lightfoot E.N., *Transport phenomena 2nd ed*. John Wiley & Sons Inc., 2002.
[16] Springer T.E., Zawodzinski T.A., Gottsfeld S., *Polymer electrolyte fuel cell model*, Journal of Electrochemical Society, vol. 138, 1991, 2334-2341.